
mKLF5 cDNA	ATGCCCACGCGGGTGTGACCATGAGCGCCCGCCTGGGACCACTGCCCCAGCCGCGGCGCG GCAGGACGAGCCCGTGTTCGCGCAGCTCAAGCCGGTGTGGGCGCTGCGAACCCGCGCCGCG ACGCGGCGCTTCTCCGGAGACGATCTGAAACACGCGCACCACCACCCGCTGCGCCGCG CCAGCCGCTGGCCCGGACTGCCCTCGGAGGAGCTGGTCCAGACAAGATGTGAAATGGAGAA GTATCTGACCCCTCAGCTCCCTCCAGTTCGATAATTTAGAGCATAAAAAGTATAGACGAG ACAGTGCCTCAGTGGTAGACCAGTTCCTCACTGACACTGAAGGCATACCTTACAGCATCAAC ATGAACGTCTTCTCCCTGACATCACTCACCTGAGAAGTGGCCTCTACAAATCCAGAGACC ATGCGTAAACACAGATCAAGACAGAACTGTTACCATTTTCAGCCACCAGAGCGAGTCGACGG CCCCTCCTCCTCCTCCGGCCCCCACCAGGCTCTCCCCGAGTTCAGTAGTATCTTCAGCTCC CACCAGACCACAGCGCCACCACAGGAGGTGAACAATATCTTCATCAAACAAGAACTTCCTAT ACCAGATCTTCATCTCTGTCCCTTCCAGCAGGGCCACCTGTACCAGCTGTTGAATACAC CGGATCTAGACATGCCAGTTCGACAAAACCAGACGGCAGTAATGGACACCCCTAATGTTTCT ATGGCAGGCCTTAACCCACACCCCTCTGCTGTTCCACAGACGTCAATGAAACAGTTCAGGG CATGCCCCCTTGACGTACACCATGCCAAGTCAGTTTCTTCCACAGCAGGCCACCTACTTTC CCCCGTCACCACCAAGCTCAGAGCCTGGAAGTCCCGATAGACAAGCTGAGATGCTGCAGAA CTCACCCACCTCCGTCCTATGCCGCTACAATTGCTTCCAAACTGGCGATTCAACACCCAAA TTTACCTGCCACTCTGCCAGTTAATTCGCCAACTCTCCACCTGTCAGATACAACAGAAGGA GTAACCCGGATCTGGAGAAGCGACGTATCCACTTCTGCGATTATAATGGTTGCACAAAAGTT TATACAAAGTCGTCTCACTTAAAAGCTCACCTGAGGACTCATAACGGGCGAGAAGCCCTACA GTGCACCTGGGAGGGCTGCGACTGGAGGTTTGCCCGGTCGGATGAGCTGACCCGCCACTACA GGAAGCACACGGGCGCAAGCCGTTCCAGTGCATGGTGTGCCAACGCAGCTTCTCCGCTCC GACCACCTCGCGCTGCACATGAAGCGCCACCAGAAC
------------	---

Table S1. The sequences of plasmids and lentiviruses.

Table S2. The primers sequences of mRNA.

Name	Forward sequences	Reverse sequences
mPTGS2	CATCCCCTTCCTGCGAAGTT	GGCCCTGGTGTAGTAGGAGA
mGAPDH	AGGTCGGTGTGAACGGATTTG	GGGGTCGTTGATGGCAACA

Table S3 Genes related to KC-IS

Cancer promoting inflammatory genes	Cancer inhibitory inflammatory genes
IL17RE	CD28
RAC3	CD4
CNTF	PLA2G2D
PLA2G4A	CRTAM
PTGS2	CD3E
ALOX12	CARD11
	RASAL3
	ZAP70
	EBI3
	TBX21
	IKZF1
	EOMES
	LCK
	CD3G
	CD8A
	THEMIS
	CD3D
	CD27
	ITK
	LEF1
	FLT3
	IRF4
	PTGER4
	SLAMF6
	KLRK1
	CD96
	CD226
	CD2
	IL1RL1
	CD247
	IL16
	NLRC3
	CCL17
	CCL22
	CXCL13
	XCR1
	CCR7

CXCR3
CXCR6
CX3CR1
LIFR
TNFSF8
CCRL2
STAP1

Table S4 | Patient characteristic

Clinicopathological parameters	NO. of cases N=67
Survival time (months)	38.1±12.7
Age at diagnosis, y	
< 60	23
≥ 60	44
Gender	
male	34
female	33
Size (largest diameter,cm)	
≤5	26
> 5	23
unknown	18
Location	
Ascending/Transverse	39
Descending/Sigmoid	28
Lymph node metastasis	
negative	45
positive	22
AJCC clinical stage	
0	1
1	6
2	30
3	21
4	3
unknown	6
Recurrence	
no	56
yes	11
KLF5	
negative	10
positive	57
CD8	
negative	43
positive	24

Figure S1. Related to Figure 1.

(A) Schematic of the experimental setup. (B) The expression of Klf5 was screened in multiple tumor cells. (C-E). The Klf5 level in PyMT-induced tumor cells was verified by Western blotting (C); representative images of tumors are displayed in (D); tumor sizes are quantified in (E). (F-H) Klf5 expression was silenced by siRNA lentivirus in EMT6 cells. Furthermore, the levels of Klf5 and its target gene cyclin D1 were verified by Western blotting (F). Representative images of tumors are displayed in (G). Tumor sizes are quantified in (H). (I-K) 67NR cells were transfected with lentivirus carrying Klf5. The levels of Klf5 and its target gene CyclinD1 were then verified by Western blotting (I); representative images of tumors are displayed in (J); tumor sizes are quantified in (K). Plot of tumor size (means \pm SD) (*p < 0.05 or ns, not statistically significant vs. control; Student's t test).

Figure S2. Activation of Klf5 is associated with an immunosuppressive microenvironment.

BALB/c mice were inoculated with control or Klf5-overexpressing (OV) 67NR cells. These tumors were collected for RNA transcriptional sequencing when they grew to approximately 1 cm. (A) Volcano plot of differentially expressed genes in Klf5-overexpressing versus control 67NR tumors. Significant gene expression with changes > 1.5-fold and P < 0.05 was considered. (B) Gene Ontology (GO) analysis was performed on transcriptional profiles for Klf5 OV vs. control groups. (C) Heatmap of the differential expression of immune-related genes in Klf5-overexpressing versus control 67NR tumors. (D) The Xcell method was performed to define the immune cell populations in Klf5-overexpressing versus control 67NR tumors. Significantly activated molecules or cell populations are highlighted in red. *p < 0.05.

Figure S3. Related to Figure 3.

(A) Western blot analysis of KLF5, CyclinD1 and COX2 in both KLF5-deficient and control HCC1806 cells. (B) HEK293T cells were cotransfected with COX2 (-1100/+100)-luc or COX2mut (-1100/+100)- luc plus PCDH-KLF5 or control vector PCDH and the internal control plasmid pRL-TK. (C-D) HCC1806 cells were subjected to the ChIP assay using the anti-KLF5 antibody or control goat IgG. PCR was performed to amplify regions surrounding the putative KLF5 binding region and a nonspecific KLF5 binding region. (E) Relative Ptges mRNA expression in control and Klf5-deficient EMT6 cells. (F) Relative Ptges mRNA expression in control and Klf5-overexpressing 67NR cells. (G) Western blot analysis of Klf5 and Ptges in both Klf5-deficient or control EMT6 and Klf5-overexpressing or control 67NR cells.

Figure S4. Blocking the Klf5/Cox2 axis synergizes with the efficacy of anti-PD1 therapy in a colon cancer model.

(A) Schematic of the experimental setup. The mice received the mentioned treatments when tumors were approximately 20 mm² in mean area. Growth curves (mean ± SEM), tumor size distributions at Day 23, individual tumor growth curves and survival curves are shown. n ≥ 4 for mice in each group. (*p < 0.05; **, p <0.01; ***, p <0.001; ****, p <0.0001 or not statistically significant vs. control; two-way ANOVA).

Figure S5. Related to Figure 6.

(A-B) Bubble heatmap of the expression of cell type-specific genes within the interface subclusters. Dot size indicates the fraction of expressing cells, colored based on normalized expression levels. (C, E) Different spatial distributions of KRT14, KRT17, KRT5, KLF5, CD4 and CD8 were overlaid onto tissue spots from our previous study or public dataset. (D) Immunohistochemical images of KLF5, COX2 and CD8 in the ST sample from our previous study. (F) Box plots show the enrichment scores of the basal signature, CD4 signature and CD8 signature in the KLF5^{high} and KLF5^{low} groups from the public dataset.

Figure S6. Related to Figure 7.

(A) Expression of KLF5 and PTGS2 in TNBC subtypes as defined in a previous study. (B) Enrichment of Gene Ontology (GO) analysis to estimate the biological processes in transcriptional profiles for KLF5^{low} vs. KLF5^{high} groups. (C-D) The levels of Klf5 and Cd8 were quantified by ImageJ after staining with specific antibodies in paraffin-embedded samples obtained from 67 patients with colon cancer. Representative images of Klf5 and Cd8 (B). The scale bar indicates 50 μ m. (C) Kaplan–Meier survival analysis of patients in the double-positive group versus the double-negative group.

Figure S1

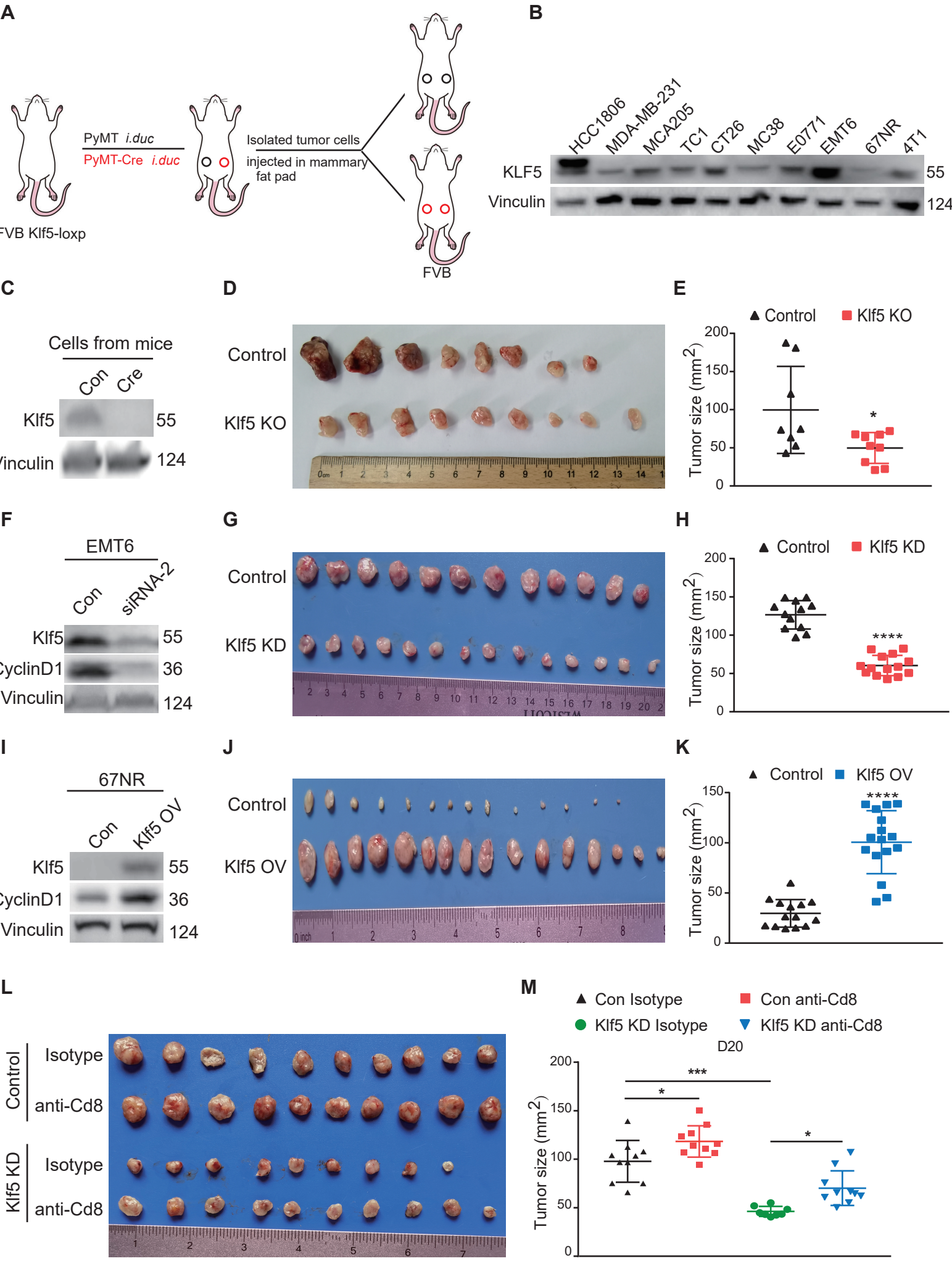


Figure S2

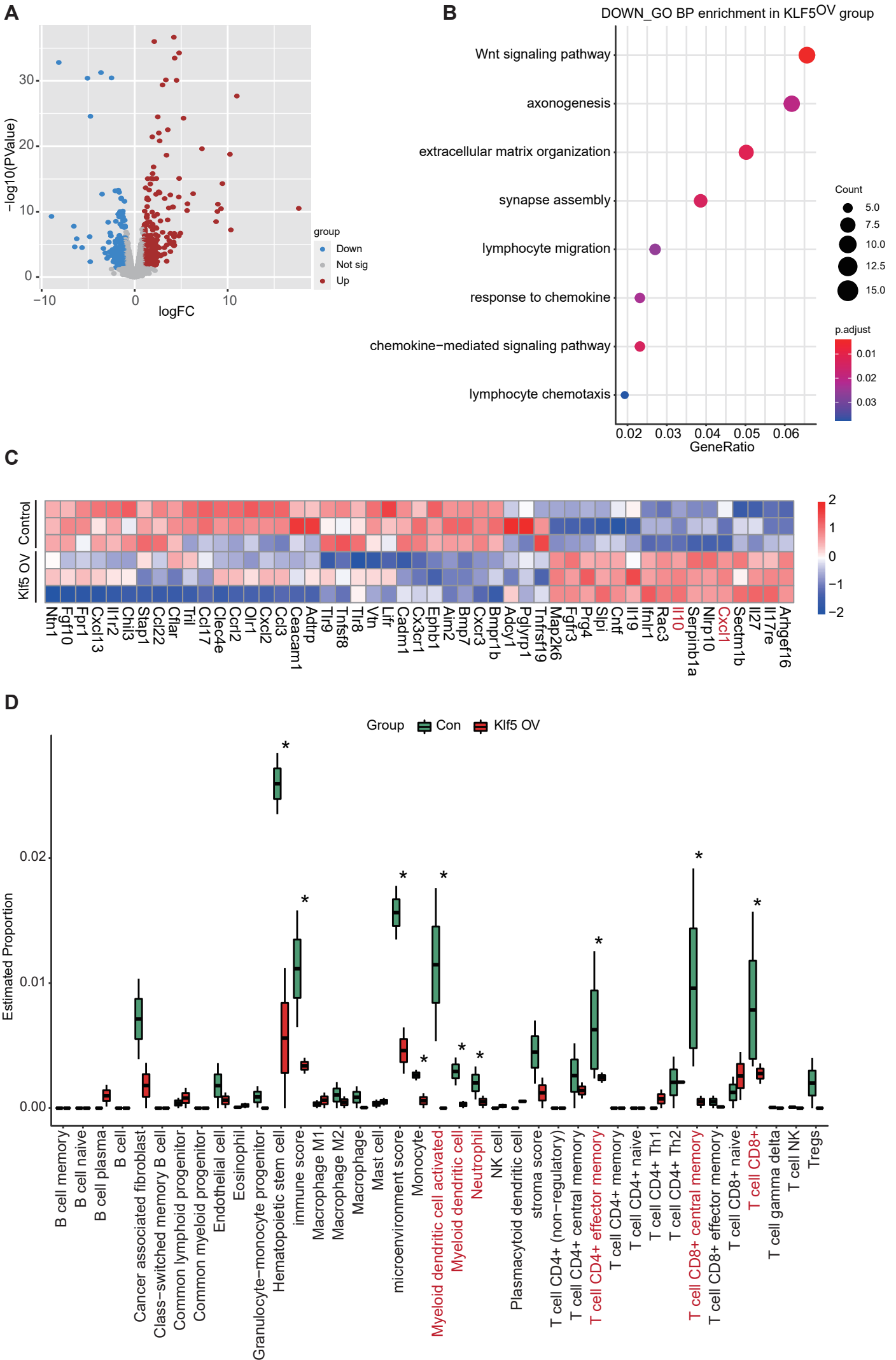
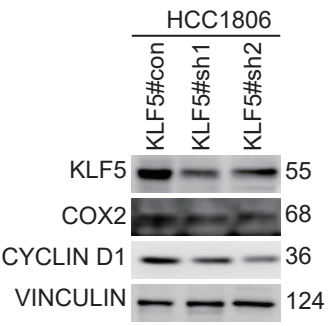
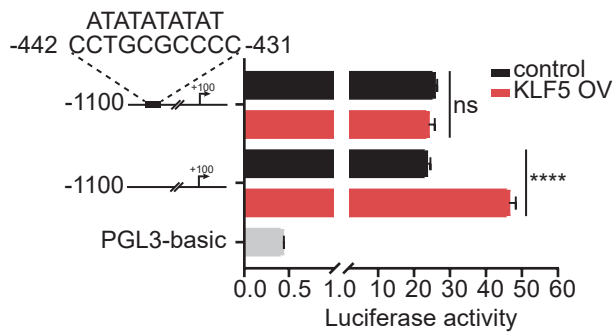


Figure S3

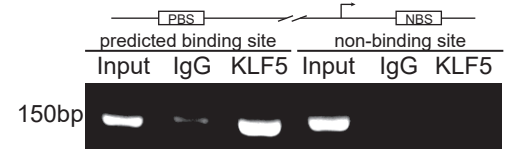
A



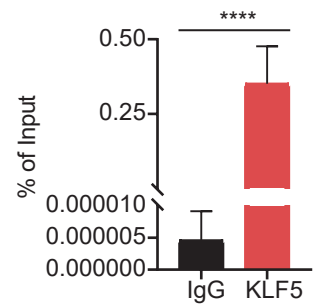
B



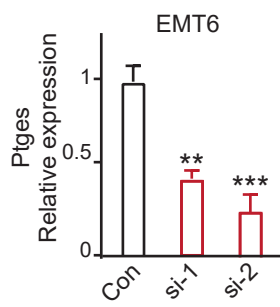
C



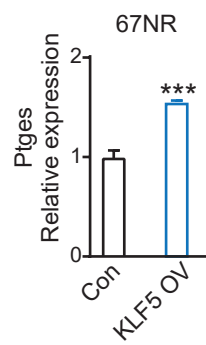
D



E



F



G

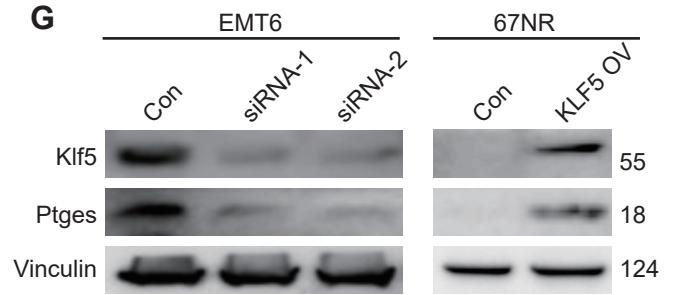


Figure S4

A

▲ Con ■ anti-Pd1 ● FZU00,004 ▼ FZU00,004+anti-Pd1 ◆ CEL ● CEL+anti-Pd1 ★ Klf5 KD ○ Klf5 KD+anti-Pd1

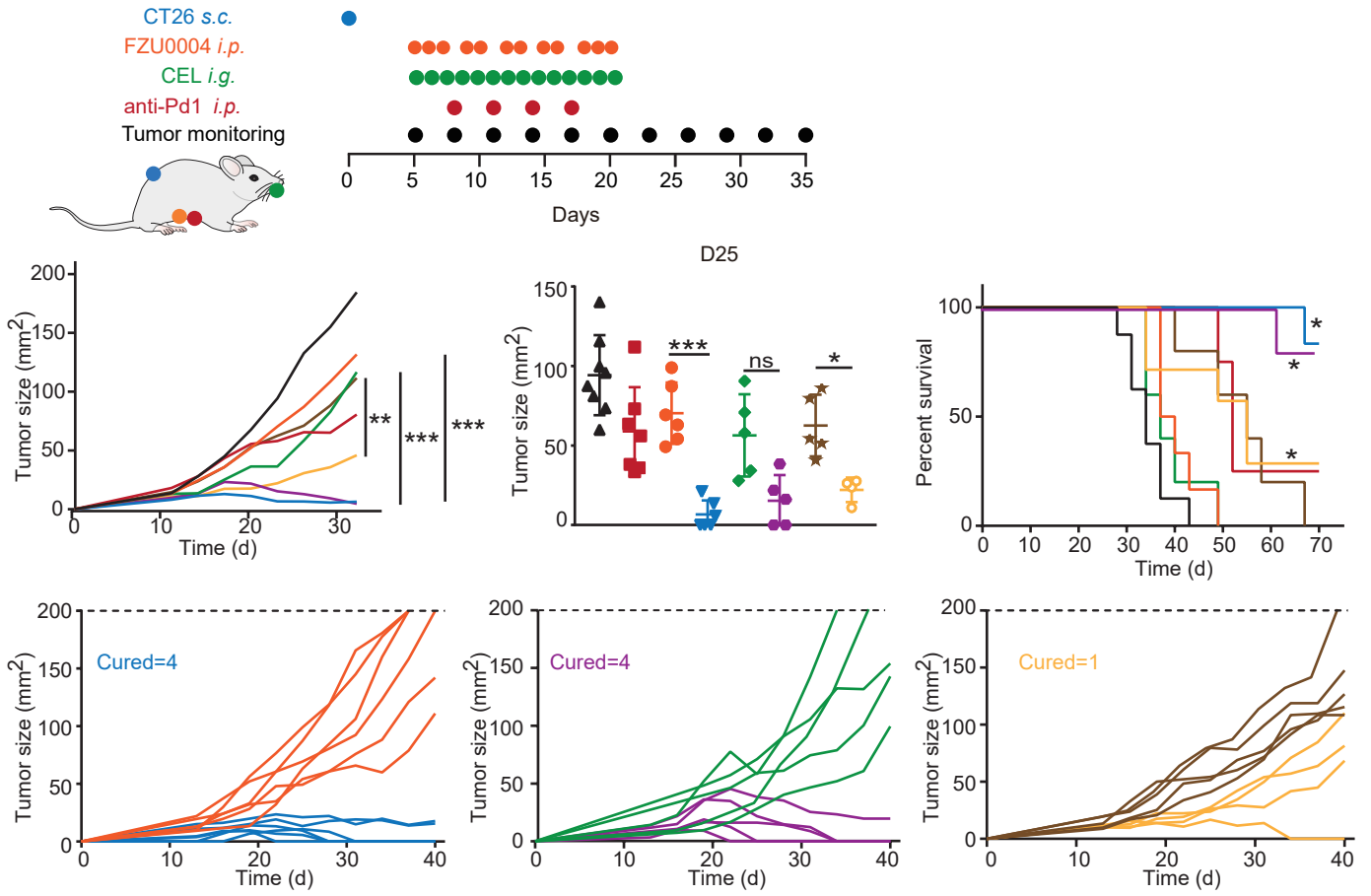


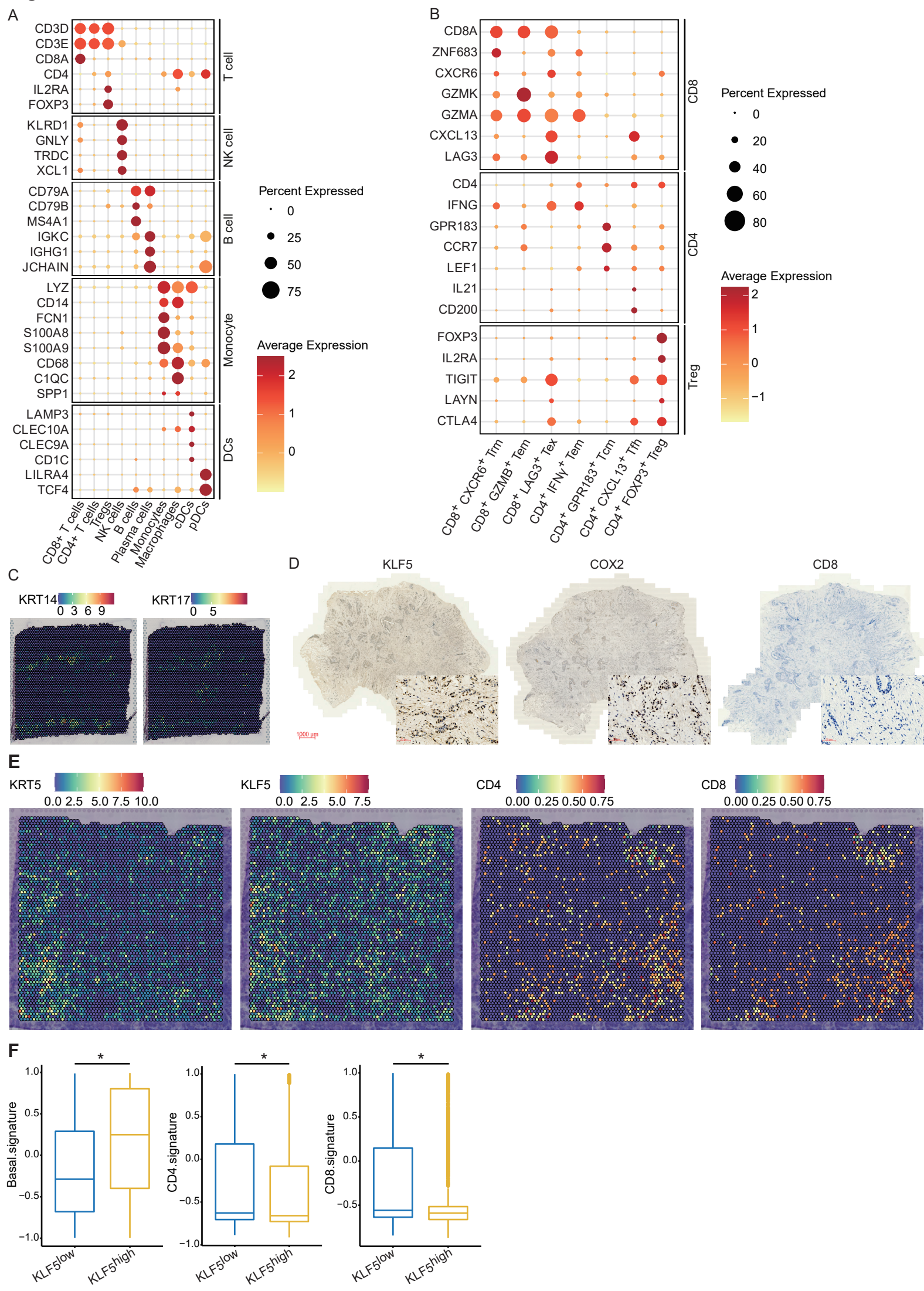
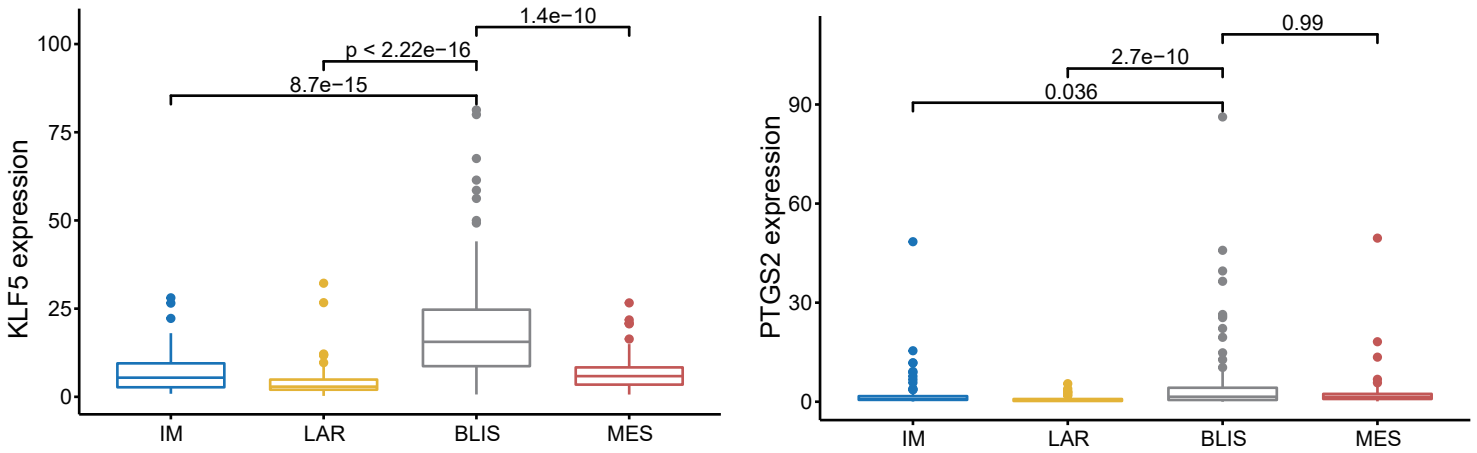
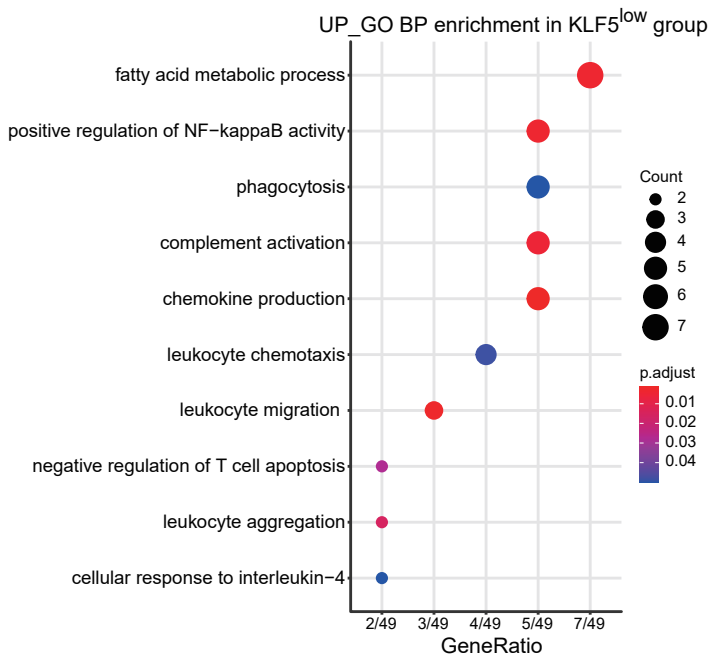
Figure S5

Figure S6

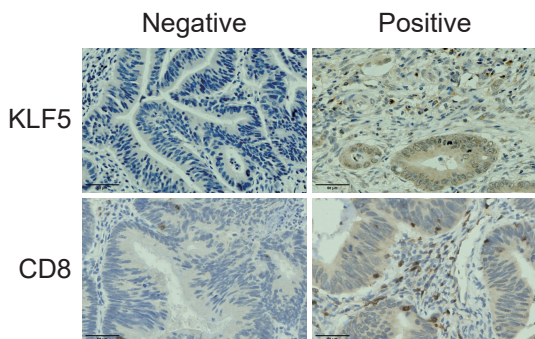
A



B



C



D

